Since January 2020 Elsevier has created a COVID-19 resource centre with free information in English and Mandarin on the novel coronavirus COVID-19. The COVID-19 resource centre is hosted on Elsevier Connect, the company's public news and information website.

Biosensors and Bioelectronics 186 (2021) 113286

Contents lists available at ScienceDirect

Biosensors and Bioelectronics

journal homepage: www.elsevier.com/locate/bios

An intelligent face mask integrated with high density conductive nanowire array for directly exhaled coronavirus aerosols screening

Qiannan Xue [1], Xinyuan Kan [1], Zhihao Pan, Zheyu Li, Wenwei Pan, Feng Zhou, Xuexin Duan [*]

State Key Laboratory of Precision Measuring Technology & Instruments, School of Precision Instruments and Optoelec-tronics Engineering, Tianjin University, Tianjin, 300072, China

ARTICLE INFO

Keywords:
Coronavirus
Intelligent sensor
Nanowires
Immunosensor
Aerosol

ABSTRACT

The current ongoing outbreak of Coronavirus Disease 2019 (COVID-19) has globally affected the lives of more than one hundred million people. RT-PCR based molecular test is recommended as the gold standard method for diagnosing current infections. However, transportation and processing of the clinical sample for detecting virus require an expert operator and long processing time. Testing device enables on-site virus detection could reduce the sample-to-answer time, which plays a central role in containing the pandemic. In this work, we proposed an intelligent face mask, where a flexible immunosensor based on high density conductive nanowire array, a miniaturized impedance circuit, and wireless communication units were embedded. The sub-100 nm size and the gap between the neighbored nanowires facilitate the locking of nanoscale virus particles by the nanowire arrays and greatly improve the detection efficiency. Such a point-of-care (POC) system was demonstrated for coronavirus 'spike' protein and whole virus aerosol detection in simulated human breath. Detection of viral concentration as low as 7 pfu/mL from the atomized sample of coronavirus aerosol mimic was achieved in only 5 min. The POC systems can be readily applied for preliminary screening of coronavirus infections on-site and may help to understand the COVID-19 progression while a patient is under prescribed therapy.

1. Introduction

The novel severe acute respiratory syndrome coronavirus 2 (SARS-CoV-2) has spread globally and more than 100 million cases have been recorded. Statistical studies show that SARS-CoV-2, like severe acute respiratory syndrome (SARS) and the Middle East Respiratory Syndrome (MERS) (Wu et al., 2020), is a highly lethal virus with a faster transmission speed. The transmission model clearly indicates that rapid and accurate identification of SARS-CoV-2 in the initial diagnosis can greatly help control the pandemic (Garba et al., 2020). The reverse transcription-polymerase chain reaction (RT-PCR) technique is recommended as the guideline for SARS-CoV-2 detection by the World Health Organization (World Health, 2020). However, current RT-PCR detection still requires sample collection, RNA extraction, amplification, the long processing time, requirement of a well-equipped laboratory, and expert operator may not provide the ability to detect all the suspected cases in a full outbreak (Ai et al., 2020). Moreover, recent reports show positive RT-PCR test results for patients recovered from COVID-19, which indicates the false positive with the genetic materials-based molecular bioassays (Lan et al., 2020). Thus, there is an urgent need to develop alternative methods for direct detection of viral pathogens in clinical samples, preferred with a miniaturized sensing system, which can perform Point-of-Care (POC) diagnostics anywhere and anytime (Hussein et al., 2020; Li et al., 2020).

Besides molecular diagnosis approaches, many efforts have been made to explore non-invasive bioassays for selective detection of the SARS-CoV-2 virus. Immunosensing chip functionalized with specific monoclonal antibodies against the SARS-CoV-2 spike protein has been reported for diagnostics of COVID-19 (Liu et al., 2020). However, as the viral particles are very small in size (typically around 100 nm), it is rather challenging to use current immunosensors for direct virus detection, which is due to the limited diffusion of viral particles towards the sensor surface in the typical low Reynolds number hydrodynamic conditions (Zourob et al., 2008). To improve the sensing performance, nanotechnology is emerging as one of the solutions to achieve highly sensitive viral pathogen detections. Due to the high surface area, various smart nanostructures and nanomaterials have been applied to enhance the capture and enrich the viral particles in solution and ambient air

* Corresponding author.
E-mail address: xduan@tju.edu.cn (X. Duan).
[1] These authors contributed equally to this work.

https://doi.org/10.1016/j.bios.2021.113286
Received 3 February 2021; Received in revised form 19 April 2021; Accepted 23 April 2021
Available online 3 May 2021

samples (Draz et al., 2018; Ganganboina et al., 2020; Islam et al., 2019; Leung and Sun, 2020; Lum et al., 2012; Xia et al., 2019; Yeh et al., 2016). Nanoscale biosensors, such as nanotubes (Palomar et al., 2020; Vadlamani et al., 2020), nanowires (Ishikawa et al., 2009), and 2D materials (Yang et al., 2018)) have been applied for virus direct detection without labeling. Benefitted by the nanoscale transducer, nanobiosensors have demonstrated greater sensitivity, shorter response time, and rather low power assumption, which is ideal for developing as POC devices (Kaushik et al., 2020). In a very recent report, functionalized 2D graphene was fabricated as a bioFET for SARS-CoV-2 virus detection and a limit of detection of 200 copies/mL in clinical samples was achieved (Seo et al., 2020). However, nasopharyngeal swabs samples are still required and the collection and handling of these clinical samples may still result in contaminations and spreading of the virus.

As a typical respiratory infectious disease (COVID-19), the SARS-CoV-2 virus spreading through breath aerosolization has been proved. Studies have shown that early COVID-19 patients emit a large number of SARS-CoV-2 viral particles through breathing, coughing, talking, or sneezing (Dhand and Li, 2020). An appropriate face mask can be used as a simple but efficient tool to avoid human-to-human transmission. For example, N95 masks are widely recommended for prophylaxis against inhaled viral aerosols. These masks use permanently charged electret fibers as the filtering medium, and in vitro experiments have revealed that they collect 95% of the aerosolized particles. It was also reported that exhaled breath collection through a face mask could provide a least invasive and convenient way for sampling the pathogens (Pleil et al., 2018). In contrast to nasopharyngeal swabs, breath sampling does not require trained medical personnel or privacy, does not create potentially infectious wastes, and can be done essentially anywhere in any time frame.

In this work, we designed and developed an intelligent face mask as a POC system, where a nanoscale impedance immunosensor composed of high density conductive nanowire arrays, a miniaturized impedance circuit including A/D converter, operational amplifier, and wireless transmission units were embedded (Fig. 1). The spacing of the nanowires is designed to match the size of the virus aerosol, which enables a highly efficient capture of the target. The impedance signals will be changed if target viral particles were detected through specific biorecognitions. Through the integrated miniaturized impedance circuit and Bluetooth module, the results can be wirelessly transmitted to a smartphone. The nanowire array is fabricated on a flexible plastic substrate by a nanoscale soft printing approach, which largely reduces the cost and facilitates the attachment to the face mask. As a POC device, the face mask is used as an enrichment apparatus of viral particles and the designed high density nanowire arrays could efficiently trap and collect the exhaled viral aerosols in a subtle way within only several minutes. The POC device is applied to detect spike proteins and gastroenteritis virus (coronavirus mimics) in diluted aqueous solution and simulated breath aerosols. Considering the rather small in size, fast response, and ultra-low power consumption benefited by the nanowires, the developed miniaturized impedance biosensor is intuitive to use, safe, simple, non-invasive, suitable for a wide range of people, easily stored, and inexpensive. The combination of a face mask with nanoscale sensors provides an affordable and sensitive POC tool with a wide range of applications in the diagnosis and management of respiratory infections.

2. Material and methods

2.1. Sensor design

We designed the nanosensor as a disposable device, which can be embedded in regular face mask specifically with N95 requirements, a typical mask version for everyday use. As shown in Fig. 1a, the nanoscale sensor contains three layers: the outside layer is a polycarbonate (PC) porous membrane, whose functions as droplets collection and sensor protection; the nanowire array with bio-functional groups as the

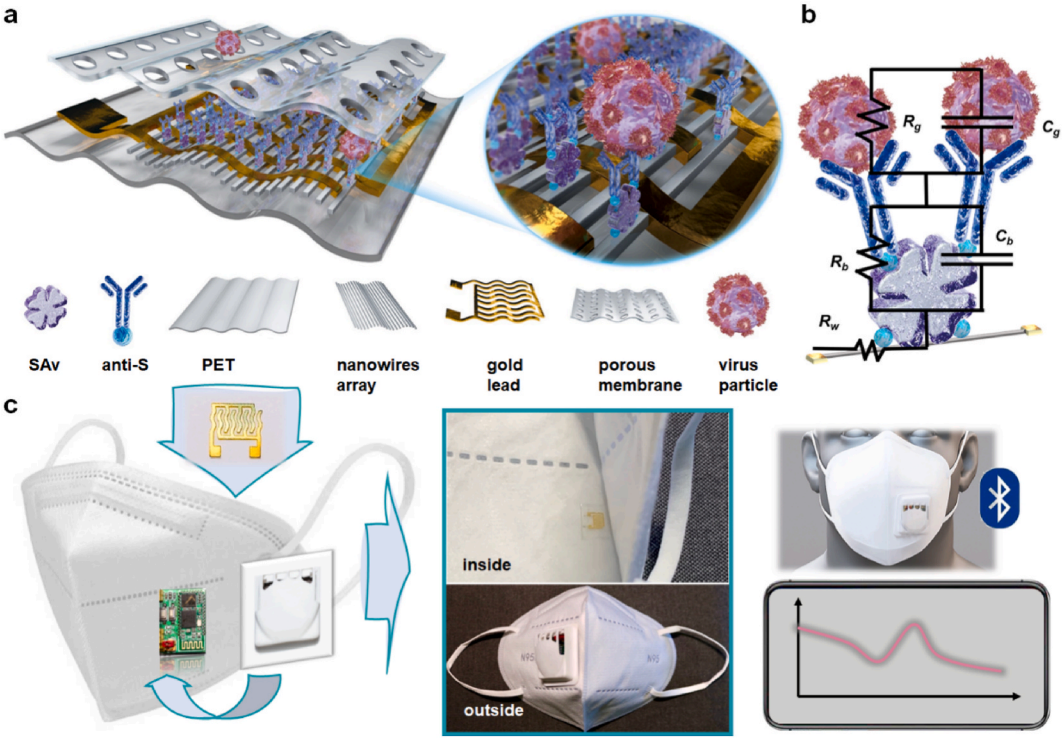

Fig. 1. Schematic illustration of the nanoscale sensor design, includes PET, nanowires array, gold lead, Sav, anti-S, porous membrane, and virus particle a), virus sensing mechanism (R_b: the equivalent resistance of surface binding antibody; R_c: the equivalent capacitance of surface binding antibody; R_g: the equivalent resistance of surface binding antigen; R_g: the equivalent capacitance of surface binding antigen; R_w: the equivalent resistance of nanowires) b), the images of the constituted intelligent face mask c). (For interpretation of the references to colour in this figure legend, the reader is referred to the Web version of this article.)

sensitive layer is in the middle; considering the curved surface of the face mask, a flexible polyethylene terephthalate (PET) substrate is used as the bottom supporting layer to facilitate the adhesion between the sensor and the mask. Regarding the design of the sensor, a few important aspects need to be addressed such as the wetting of the surface, the dimensions of the electrodes, the bio-conjugation steps, and the stability of the sensors, which all involve the viral particles capture efficiency and sensor performance.

i) As the surface of the face mask is rather hydrophobic, hydrophilic porous PC membrane was applied here as a surface energy trap to collect and enrich the respiratory droplets (Tucker et al., 2020). Considering the size distribution of the typical viral particles in the exhaled breath is approximately 100–300 nm (Leung and Sun, 2020), the pore size of the membrane was set as 400 nm, which can prevent larger particles encountering to the bottom sensitive nanowire interface, Besides, the porous membrane also reduces the jet velocity of the breathed aerosol, avoiding the direct impact of the airflow to the sensor stability.
ii) The nanowires array was designed to parallel patterned on the substrates and vertically connected with the gold interdigitated electrodes (IDT). The width and spacing of the nanowires were set both as 75 nm (Fig. 1a). Such high density nanowire arrays allows higher collision frequency between the immobilized antibodies and target antigens, thus ensuring the efficient capture of the nanoscale viral aerosols (Campos et al., 2020). Besides, the increased surface area by the nanoscale electrodes improves the sensitivity as well as signal to noise ratio of the sensor (Liu et al., 2017). The molecular design of the bio-ink was introduced in detail in our previous work (see also the Supplementary Materials S1) (Xue et al., 2019). Poly (3,4-ethylenedioxythiophene) polystyrene sulfonate (PEDOT:PSS) is negatively charged and polyelectrolytes (PLL-*g*-OEG4-Biotin) is positively charged, which leads to the direct formation of bio functionalized nanowires without multiple post modification steps (Figure s1). The introduced PEG groups provide a nonfouling surface which can increase the selectivity of the sensor. The proposed bio-ink is water-soluble, thus it can be directly patterned using low-cost soft printing approach without requirement of the cleanroom. For coronavirus detection, antibodies studies have shown that spike proteins (S-protein) from SARS-CoV-2 have greater reactivity (Shang et al., 2020). Thus anti-spike proteins were used in this work. The directly doped biotin groups on the surface of nanowires facilitate the immobilization of the anti-spike proteins through the specific streptavidin (SAv)-biotin interactions.
iii) PET was selected as the bottom layer of the sensor considering its water proof but gas permeability. Considering the device is mounted inside of a face mask, thus the bending of the device cannot be avoided. In order to conform to the face mask, the metal electrode was designed as a snake shape for maintaining its conductivity under bending conditions. The three layers of the sensor are all flexible, which makes the proposed sensor has good shape compliance.

Materials and reagents used were shown in Supplementary Materials S8.

2.2. Sensing principle

The sensor is constructed as a non-Faradic impedance biosensor to enable a label-free virus particles detection through the specific antibody-antigen immuno-interactions. The detection principle of the immunosensor is in accordance with the impedance model (Fig. 1b). The surface binding antibody can be simulated by the resistance R_b and capacitance C_b in parallel. After the target viral particles are captured, the surface is equivalent to the impedances of antigens, that R_g is parallel to C_g. The nanowires between the two contact electrodes exhibit pure resistance behavior, which could be simulated by the series resistance R_w. It conforms to a series equivalent circuit model (Yao et al., 2017), which is shown in eq. (1).

$$|Z_t| = |R_w| + |R_b \Big/ \Big/ \frac{1}{j\omega C_b}| + |R_g \Big/ \Big/ \frac{1}{j\omega C_g}| \quad \text{(eq.1)}$$

Therefore, the amount of target antigens adsorbed on the nanowires, increases with an increase in the sample concentration, which leads to an increase in the impedance of antigens captured, $|Z_g| = |R_g \Big/ \Big/ \frac{1}{j\omega C_g}|$, and leads to an increase in the measurement impedance, $|Z_t|$.

2.3. Intelligent face mask construction

To develop as a POC device, a miniaturized impedance circuit was designed to embed on the outside of the face mask, which was connected with the sensor through silver wires. The impedance circuit is used to convert the sensing signals from the nanowires to digital data and transmit wirelessly to a smartphone (Fig. 1c). It has an A/D impedance module, an operational amplifier, and a Bluetooth wireless transmission unit. The circuit size is less than $2.5 \times 3.5 \times 0.5$ cm^3, which matches the size of the regular respiration valve of typical N95 mask. A smart phone compatible APP was developed as well to display and analysis the sensing signals in real-time. Since the impedance circuit is not exposed to pollutants, it can be simply recycled and reused.

Overall, the design of the intelligent face mask as a wearable device for the rapid on-site screening of exhaled coronaviruses particles has the advantages of low cost and high compatibility with existing manufacturing methods. It can meet the large needs of requirements for preliminary screening of the coronavirus infections, such as in airport, at customs control etc. The wireless communication can be adapted to artificial intelligence (AI) to acquire maximum information from the response allowing mask wearer to make a quick decision.

3. Results and discussion

3.1. Fabrication and characterization of the nanowire array-based immunosensor

The nanowires were fabricated on PET substrate using the nanoscale soft printing approach. A nanoscale soft model based on polydimethylsiloxane (PDMS) and mr-I T85 (Microresist) was prepared using a thermal imprint to form nanogroove structures (Tang et al., 2019). Nanochannels were formed by soft bonding the nanogrooves with the PET substrate. The rather large Laplace pressure facilitates the bio-ink filling to the channels. The design of the bio-ink and detail fabrication process of the nanowires were shown in Supplementary Materials S1. After removing the soft mode, PEDOT:PSS nanowires doped with the biotin groups corresponding to the width of the nanochannels were patterned on the flexible substrate.

Fig. 2a shows the AFM (Atomic Force Microscope) height image of the original silicon template. Fig. 2b and c shows the AFM height and 3D images of the patterned PEDOT:PSS nanowires on the PET substrate. The nanowires are uniformly patterned and parallel to each other. The width and spacing of the nanowires are approximately 75 nm (Fig. 2d), which is consistent with the size of the template. Unlike the disordered nanowires, where sensitive sites readily overlap with each another, the parallel patterned nanowire arrays minimize the steric hindrance for target capturing and ensures the device repeatability from different batch. In particular, considering the size of the viral aerosol is larger than 100 nm, the high density sub-100 nm nanowire arrays ensures the efficient capture of the individual viral particle by the nanowires.

The electrical behavior of the sensor was then characterized by an electrochemical impedance spectroscopy with a two electrodes configuration. The nanowires-based sensor was detected by the B1500A,

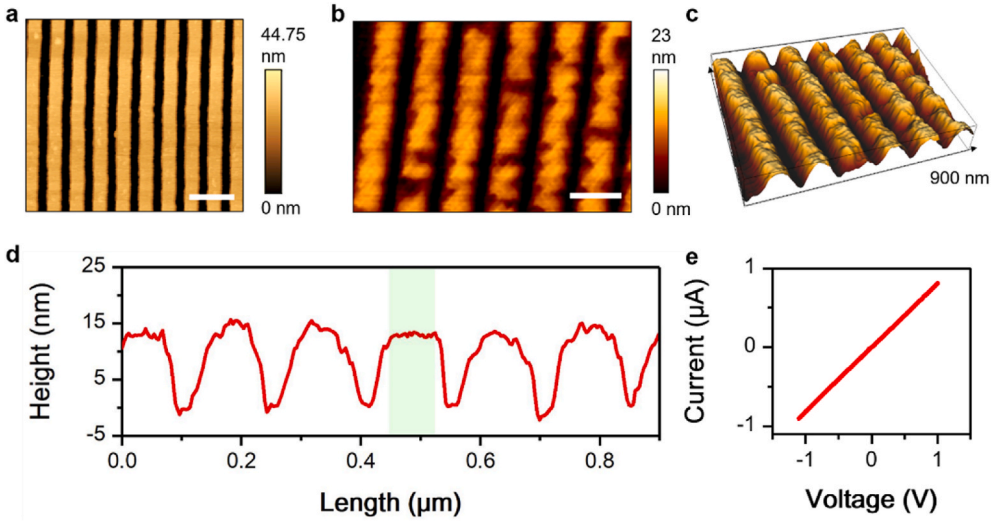

Fig. 2. AFM surface morphology analysis of the silicon mode a); the nanowires fabricated on a PET substrate b); the three-dimensional AFM image of the nanowires c); the height information of the nanowires (The width of the light green box is 75 nm) d); The relation between current and voltage of nanowires fabricated on flexible substrates by nanoscale printing technology e). Scale bar in the image denotes 200 nm. (For interpretation of the references to colour in this figure legend, the reader is referred to the Web version of this article.)

Keysight for Current–voltage (I–V). IV measurements were performed using a voltage sweep of −1 to +1 V between the two metal electrodes of the PEDOT:PSS nanowires. When the voltage is applied to both ends of the nanowires, the conductivity of the nanowires showed a typical Ohm's behavior and the current increases linearly. The result shows that the nanowires are purely resistive with linear conductivity and have good continuity in the sensing area (Fig. 2e). The resistivity of the nanowires was calculated as 5.6×10^{-1} Ω m, which is consistent with the geometry design of the nanowires array (see also Supplementary Materials S2). These results prove that the good quality of the fabricated nanowires array. Next, the immobilization of the SAv and anti-spike proteins were checked by the impedance measurement. As shown in Figure s2b, as the SAv and antibodies were linked to the nanowires, the corresponding impedance increased successively, indicating the proposed biosensor can detect protein adsorption on the surface of the nanowire by recording the change in the impedance spectrum and the antibodies are successfully immobilized on the nanowires. The lifetime of the sensor depends on the immobilized antibodies. We stored the sensor at room temperature for three days and no degradation of the sensing performance was observed. For longer storage, it is recommended to refrigerate it at 2–8 °C.

We then tested the bending effect to the sensor performance. The impedance response of the sensor in flat and bended (∠15°) states were recorded. As shown in Figure s2e, slight bending hardly affects the impedance response of the device.

3.2. Spike protein detection in solution

After immobilization of the anti-S protein, the nanoscale impedance device was tested for S protein sensing. The good conductivity of the PEDOT:PSS nanowires makes it possible to measure its impedance at low frequency range with low background signal. We used electrochemical workstation (Versa STAT 4 electrochemical workstation, USA) to record the impedance spectra of the sensor from 1 to 9 Hz both at dry and wet conditions. In all impedance measurements, the recommended amplitude is not more than 1 V (Gao et al., 2018). Here, measurements were completed with voltage amplitude of 200 mV at room temperature. Fig. 3a shows the impedance magnitude of the nanowire in dry state. After dipping in liquid, a change of the impedance spectrum was observed (Fig. 3b & Figure s4a). The decrease of the impedance which is

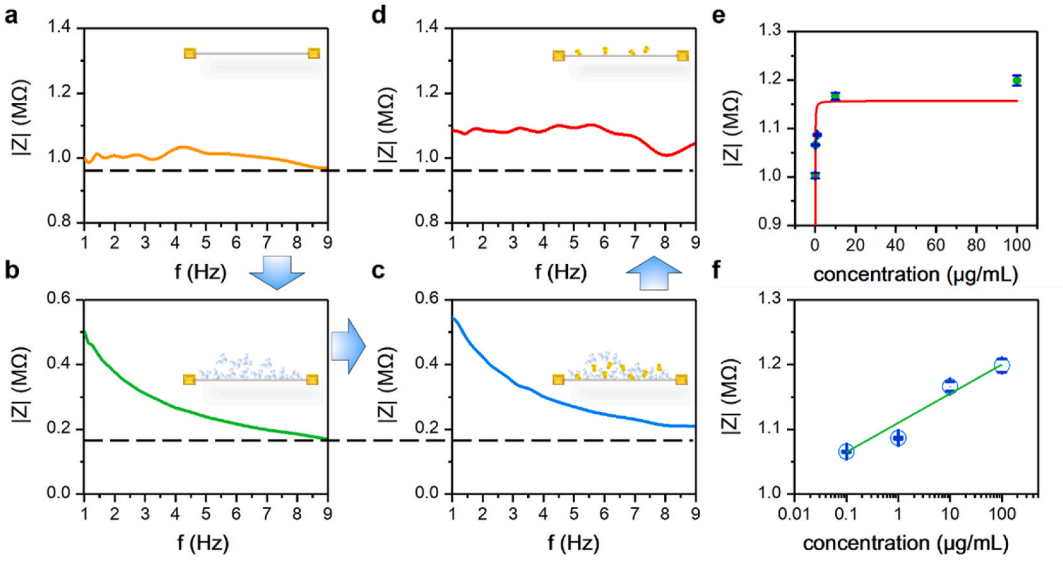

Fig. 3. The impedance spectra of nanowire-based immunosensor before a) and after wetting b); after contact the solution containing the spike protein in wet c); and under dry conditions d); The insert graph is the schematic diagram of nanowire binding protein. The impedance value plotted with different concentrations of the spike protein e) and in log (μg/mL) f). The slope is 0.048 MΩ/log (concentration).

likely due to the swelling of the humidity-sensitive PSS particles in the nanowires (Zhou et al., 2020). The impedance signal was increased by contacting with the S protein solution (0.1 μg/mL) (Fig. 3c & Figure s4b). Fig. 3d shows the impedance spectrum of the nanowire device after completely dried. The impedance value is again significantly higher than that without contact with the S protein (Fig. 3a), indicating that the antibody functionalized the nanowires can successfully capture the S protein in solution. The above results show that the prepared nanowire-based immunosensor can detect whether the S protein is bound on the nanowire surface by measuring the impedance spectrum.

Next, different concentrations of spike proteins (0.1 μg/mL to 100 μg/mL) were applied to the sensor surface. After blow drying, the impedance magnitude at 3.55 Hz was plotted in Fig. 3e. The frequency of 3.55 Hz was found to have the highest linearity in the frequency range of 1–9 Hz (Figure s4c). The results show that the impedance magnitude increases with an increase in the protein concentration. The impedance values detected by the sensor at each concentration were averaged after three measurements. The data from Fig. 3e was fitted with Langmuir equation, the affinity constant K_d for S protein is calculated about 1.8 nM, which is close to the reported value (Chi et al., 2020). As shown in Fig. 3f, linear logarithmic relationship was found between the impedance change ($R^2 = 0.951$), ΔZ in MΩ, and the protein concentration, in log (μg/mL), and the limit of detection was determined to be 0.02 μg/mL (3δ/Sensitivity). The above results confirm that the prepared nanowire-based immunosensor can detect whether the spike protein is bound on the nanowire surface by measuring the impedance spectrum. It is also observed that the impedance values begin to plateau after incubation of S-protein at 10 μg/mL, which suggests the saturation of the sensor surface.

3.3. Face mask integration and exhaled protein detection

After detection of the S protein in spiked solution, we integrated the nanosensor in a real face mask and tested its performance for exhaled sample detection. The sensor is placed inside of a face mask, which is located opposite of the nose and mouth region to facilitate the direct capture the exhaled virus aerosol (Fig. 4a). A miniaturized impedance circuit is mounted on the outside of the face mask, which is connected to the flexible sensor through two silver wires (Fig. 4b). It contains an AD5933 chip, which can collect the impedance values, an operational amplifier AD820 chip, a central processing module and a Bluetooth module (Fig. 4c). The power supply is provided by a 3.6 V button battery. The circuit design architecture is shown in Figure s5a. Figure s5b shows the calibration curve of the miniaturized impedance circuit for standard components. The circuit size is designed to be less than 2.5 × 3.5 × 0.5 cm^3 and the weight is 7.6 g, which can be easily mount to the face mask and will not affect the wearable comfortability (Figure s5e&s5f). The collected impedance spectrum can be wirelessly transmitted to a smartphone via Bluetooth and is displayed using a specific application (APP) in real-time (Fig. 4d). A customized nebulizer (model TK-3, Kanghua, Changzhou, China) is used to atomize the solution containing spike protein sample. The aerosols were expelled into the face mask through the throat of the dummy to simulate human exhalation.

As shown in Fig. 4e, initially, the sensor was in a dry state. After blank solution was applied, the impedance value increased. We also observed that the impedance value reaches the maximum value after 5 min atomization which indicates that the humidity in the face mask is stabilized then. After blow drying the face mask, the impedance value went back to the original level. This proves that if the exhaled air vapor does not contain target S proteins, the response will not be changed. 1 ng/mL and 10 ng/mL of S protein solution was added in the nebulizer, after 10 min atomization under the same conditions, the impedance spectrum was collected by the smartphone APP (Fig. 4f). The calculated impedance value at 7 Hz was significantly higher than that of the control solution and S protein with higher concentration (10 ng/mL) results higher impedance magnitude as well. These results prove that the developed nanowire sensor together with the miniaturized impedance circuit can be well performed to detect atomized protein in a face mask.

3.4. Virus aerosol detection

After successfully demonstrated for S protein sample detection, we applied the POC device for real exhaled viral particles detection. Here, porcine transmissible gastroenteritis virus (TGEV) was applied as a coronavirus aerosol mimic since it contains spike membrane proteins and will not infect human. TGEV has an aerodynamic diameter of approximately 120 nm (Riquelme et al., 2002) which is widely used as a viral aerosol substitutes due to its robustness and morphological similarity to pathogenic viruses (Kim et al., 2007). Here, TGEV aqueous solution (700 pfu/mL, 5 mL) was injected into a customized nebulizer and an atomizing rate of 0.3 mL/min was used for the bioaerosol sampling test. Compressed clean air was passed into the nebulizer at a flow rate of 6 L/min. The viruses could remain active in the expelled aerosols (Lee et al., 2020), and can be accumulated easily in face mask. Two concentrations of viral particles (7 pfu/mL, and 700 pfu/mL) were measured (Video S1). After 5 min exposure, the impedance data were recorded by the cell phone. Fig. 5a plots the impedance spectrum curve together with the control sample (without virus). It clearly shows that the proposed sensor can distinguish between a coronavirus-free, low and high concentration of coronavirus. The smallest distinguishable

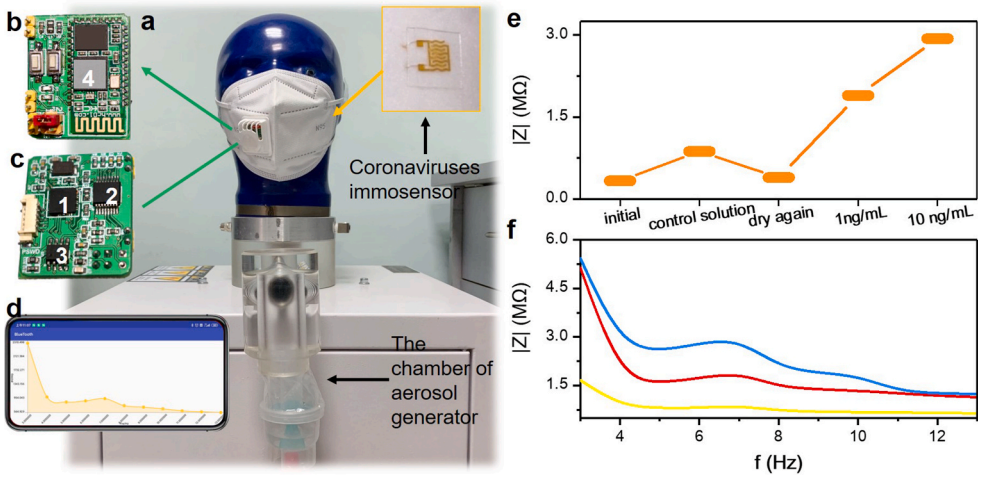

Fig. 4. The setup of the breath simulation experiment a). The top b) and back side c) of the miniaturized impedance circuit (1: STM32; 2: AD5933; 3: AD820; 4: Bluetooth model). The display of the smart phone d). Impedance peak recorded at different sensing status and contacted with two different protein concentrations e). Impedance spectra plot with different concentrations of S proteins measured in the atomized state f) (yellow: 0, red: 1 ng/mL; blue: 10 ng/mL). (For interpretation of the references to colour in this figure legend, the reader is referred to the Web version of this article.)

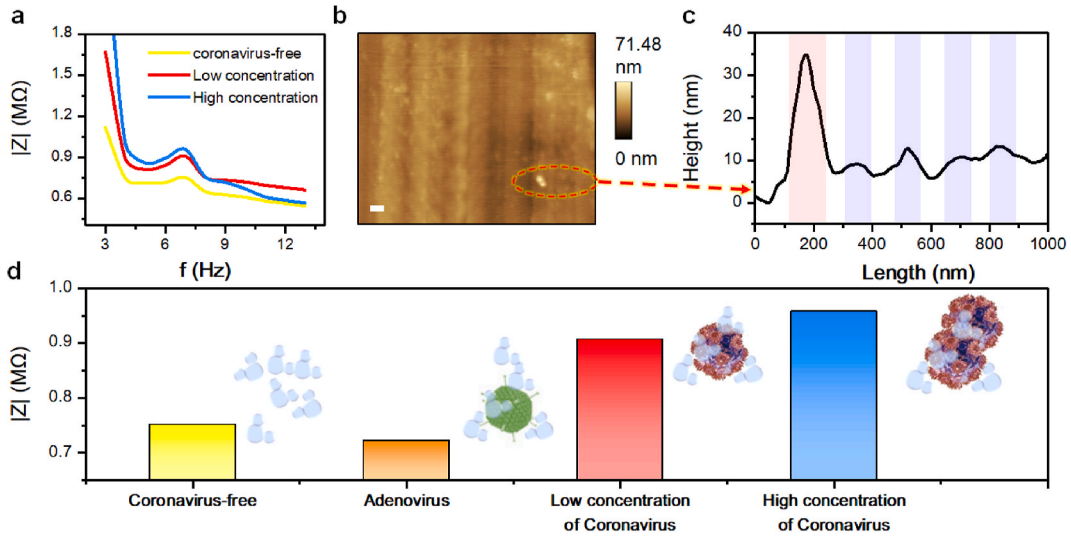

Fig. 5. Impedance spectra plot with three concentrations of coronavirus (yellow: control, red: 7 pfu/mL, blue: 700 pfu/mL) in the atomization experiment a). AFM observation of virus captured by the nanowires b) and the corresponding height profile c) (The width of the light pink box is 112 nm and the width of the light blue box is 75 nm). Scale bar in the image denotes 200 nm. The peak impedance values of three different conditions of viral particles detection (yellow: control, red: 7 pfu/mL, blue: 700 pfu/mL) and 700 pfu/mL adenovirus (orange) in the atomization experiment d). (For interpretation of the references to colour in this figure legend, the reader is referred to the Web version of this article.)

concentration is 7 pfu/mL, corresponding to an air concentration of 0.35 pfu/L, which is below the previously reported virus aerosol detection limits (e.g. $10^{4.294}$, 50% egg infectious dose (EID50)/m^3 and 1.9×10^7 pfu/L, respectively (Lee et al., 2020; Usachev et al., 2014)) and can meet the requirement to identity the early stage COVID-19 patients from their aerosols (Ma et al., 2020). The response consistency (R.S.D.) for the simulated coronavirus aerosols is less than 96.3% (Figure s6a). Compared with the protein detection, the sensor responses even faster. This is likely due to the design of the high-density sub-100 nm nanowires array, which can effectively capture even a few viral particles and larger particles actually result higher impedance change.

Supplementary video related to this article can be found at https://doi.org/10.1016/j.bios.2021.113286

AFM was then applied to visualize the captured viral particles. Fig. 5b shows that a viral particle attached on one of the nanowires with a diameter of 112 nm and 38 nm in height (Fig. 5c), which indicates the successful capture of the nanoscale viral particles by the nanowire array. To test the specificity of the sensors, Adenovirus which does not contain S-protein was applied as a control sample (Bandaly et al., 2019). 700 pfu/mL Adenovirus solution was atomized by the nebulizer at the same condition. The impedance spectrum was then recorded at the same time frame. As shown from Fig. 5d, the peak value of adenovirus (orange) is almost the same as the blank solution (yellow). These results demonstrate that the intelligent face mask can selectively detect the virus particles containing the S-protein with simulated human breathing. The sensor will have cross reactivity with other virus particles, which also contain S-protein, since it is not available of antibodies specific to the targeted SARS-CoV-2. However, the goal of the proposed antigen detection POC device is to screen large amount of people who may carrying coronavirus with S-protein quickly and conveniently, as it does not rely on target amplification. The identified positive infected people can be further checked by the regular RT-PCR, thus it can reduce the heavy loading to detect all the suspected cases by PCR in a full outbreak.

In this work, the nanowires sensor was covered by a porous membrane to prevent potential contaminations. Introduction of a reference sensor together with differential measurement circuit may be considered to further reduce other interferences. Regarding the cost, the face mask including the nanowires sensor should be disposable to prevent potential cross infections. However, the circuit embedded on the outside of the face mask can be simply recycled after disinfection. The nanowires sensor is fabricated based on batch printing process and the PEODT:PSS is rather cheap materials. Thus the cost of the sensor is low enough for one time usage.

4. Conclusions

In this work, a nanoenabled intelligent face mask has been proposed for screening breathed coronaviruses aerosols. Antibody functionalized sub-100 nm conductive nanowire array together with an impedance circuit are constructed as a miniaturized impedance immunosensor, which is small, lightweight, and enables integration with a regular face mask. The nanowires were fabricated with nanoscale soft printing, featured with low cost and mass producible. The design of the nanowires array ensures the capture efficiency of the target viral particles. The experimental results show that the proposed intelligent face mask can distinguish the coronavirus aerosols, which atomized from the solution as low as 7 pfu/mL within only a few minutes. The proposed nanowire sensor integrated face mask enables aerosol mediated diagnosis, which can detect the aerosols of coronavirus particles in a simple and unattended way. It does not require trained medical personnel, does not create potentially infectious wastes, and can be done essentially anywhere in any time frame. Especially, it can solve the problems of medical resource saturation caused by the influx of a great number of suspected cases and it is suitable for the scenarios such as customs and airports where rapid screening is required.

CRediT authorship contribution statement

Qiannan Xue: Conceptualization, Methodology, Preparation, Experiment, Analysis, Writing – original draft & revising. Xinyuan Kan: Preparation, Experiment, Circuit, Software, Writing – proofreading. Zhihao Pan: Circuit, Software. Zheyu Li: Assist in the preparation. Wenwei Pan: Protein preparation. Feng Zhou: Assist in the experiment. Xuexin Duan: Conceptualization, Methodology, Writing – review & revising.

Declaration of competing interest

The authors declare that they have no known competing financial interests or personal relationships that could have appeared to influence

the work reported in this paper.

Acknowledgments

The authors gratefully acknowledge financial support from the National Natural Science Foundation of China (NSFC No. 91743110, 21861132001), National Key R&D Program of China (2017YFF0204604, 2018YFE0118700), Tianjin Applied Basic Research and Advanced Technology (17JCJQJC43600), the 111 Project (B07014).

Appendix A. Supplementary data

Supplementary data to this article can be found online at https://doi.org/10.1016/j.bios.2021.113286.

References

Ai, T., Yang, Z., Hou, H., Zhan, C., Chen, C., Lv, W., Tao, Q., Sun, Z., Xia, L., 2020. Radiology 296, E32–E40.
Bandaly, V., Joubert, A., Andres, Y., Le Cann, P., 2019. Aerobiologia 35, 357–366.
Campos, R.K., Jin, J., Rafael, G.H., Zhao, M., Liao, L., Simmons, G., Chu, S., Weaver, S.C., Chiu, W., Cui, Y., 2020. ACS Nano 14, 14017–14025.
Chi, X., Liu, X., Wang, C., Zhang, X., Li, X., Hou, J., Ren, L., Jin, Q., Wang, J., Yang, W., 2020. Nat. Commun. 11, 4528.
Dhand, R., Li, J., 2020. Am. J. Respir. Crit. Care Med. 202, 651–659.
Draz, M.S., Lakshminaraasimulu, N.K., Krishnakumar, S., Battalapalli, D., Vasan, A., Kanakasabapathy, M.K., Sreeram, A., Kallakuri, S., Thirumalaraju, P., Li, Y., Hua, S., Yu, X.G., Kuritzkes, D.R., Shafiee, H., 2018. ACS Nano 12, 5709–5718.
Ganganboina, A.B., Khoris, I.M., Chowdhury, A.D., Li, T.-C., Park, E.Y., 2020. ACS Appl. Mater. Interfaces 12, 50212–50221.
Gao, M., Hazelbaker, M.S., Kong, R., Orazem, M.E., 2018. Electrochim. Acta 275, 119–132.
Garba, S.M., Lubuma, J.M.S., Tsanou, B., 2020. Math. Biosci. 328, 108441.
Hussein, H.A., Hassan, R.Y.A., Chino, M., Febbraio, F., 2020. Sensors 20, 4289.
Ishikawa, F.N., Chang, H.-K., Curreli, M., Liao, H.-I., Olson, C.A., Chen, P.-C., Zhang, R., Roberts, R.W., Sun, R., Cote, R.J., Thompson, M.E., Zhou, C., 2009. ACS Nano 3, 1219–1224.
Islam, S., Shukla, S., Bajpai, V.K., Han, Y.-K., Huh, Y.S., Kumar, A., Ghosh, A., Gandhi, S., 2019. Biosens. Bioelectron. 126, 792–799.
Kaushik, A.K., Dhau, J.S., Gohel, H., Mishra, Y.K., Kateb, B., Kim, N.-Y., Goswami, D.Y., 2020. ACS Appl. Bio Mater. 3, 7306–7325.
Kim, S.W., Ramakrishnan, M.A., Raynor, P.C., Goyal, S.M., 2007. Aerobiologia 23, 239–248.
Lan, L., Xu, D., Ye, G., Xia, C., Wang, S., Li, Y., Xu, H., 2020. J. Am. Med. Assoc. 323, 1502–1503.
Lee, I., Seok, Y., Jung, H., Yang, B., Lee, J., Kim, J., Pyo, H., Song, C.-S., Choi, W., Kim, M.-G., Lee, J., 2020. ACS Sens. 5 (12), 3915–3922.
Leung, W.W.-F., Sun, Q., 2020. Separ. Purif. Technol. 245, 116887.
Li, Z., Yi, Y., Luo, X., Xiong, N., Liu, Y., Li, S., Sun, R., Wang, Y., Hu, B., Chen, W., Zhang, Y., Wang, J., Huang, B., Lin, Y., Yang, J., Cai, W., Wang, X., Cheng, J., Chen, Z., Sun, K., Pan, W., Zhan, Z., Chen, L., Ye, F., 2020. J. Med. Virol. 92, 1518–1524.
Liu, W., Liu, L., Kou, G., Zheng, Y., Ding, Y., Ni, W., Wang, Q., Tan, L., Wu, W., Tang, S., Xiong, Z., Zheng, S., 2020. J. Clin. Microbiol. 58 e00461-e00420.
Liu, X., Yang, W., Chen, L., Jia, J., 2017. Electrochim. Acta 235, 519–526.
Lum, J., Wang, R., Lassiter, K., Srinivasan, B., Abi-Ghanem, D., Berghman, L., Hargis, B., Tung, S., Lu, H., Li, Y., 2012. Biosens. Bioelectron. 38, 67–73.
Ma, J., Qi, X., Chen, H., Li, X., Zhang, Z., Wang, H., Sun, L., Zhang, L., Guo, J., Morawska, L., Grinshpun, S.A., Biswas, P., Flagan, R.C., Yao, M., 2020. Clinical Infectious Diseases. an Official Publication of the Infectious Diseases Society of America, p. ciaa1283, 2020.
Palomar, Q., Xu, X., Gondran, C., Holzinger, M., Cosnier, S., Zhang, Z., 2020. Microchimica Acta 187, 363.
Pleil, J.D., Wallace, M.A.G., Madden, M.C., 2018. J. Breath Res. 12, 027110.
Riquelme, C., Escors, D., Ortego, J., Sanchez, C.M., Uzelac-Keserovic, B., Apostolov, K., Enjuanes, L., 2002. Emerg. Infect. Dis. J. 8, 869–870.
Seo, G., Lee, G., Kim, M.J., Baek, S.-H., Choi, M., Ku, K.B., Lee, C.-S., Jun, S., Park, D., Kim, H.G., Kim, S.-J., Lee, J.-O., Kim, B.T., Park, E.C., Kim, S.I., 2020. ACS Nano 14, 5135–5142.
Shang, J., Ye, G., Shi, K., Wan, Y., Luo, C., Aihara, H., Geng, Q., Auerbach, A., Li, F., 2020. Nature 581, 221–224.
Tang, N., Zhou, C., Xu, L., Jiang, Y., Qu, H., Duan, X., 2019. ACS Sens. 4, 726–732.
Tucker, B., Hermann, M., Mainguy, A., Oleschuk, R., 2020. Analyst 145, 643–650.
Usachev, E.V., Tam, A.M., Usacheva, O.V., Agranovski, I.E., 2014. J. Aerosol Sci. 76, 39–47.
Vadlamani, B.S., Uppal, T., Verma, S.C., Misra, M., 2020. Sensors 20, 5871.
World Health, O., 2020. World Health Organization, Geneva.
Wu, Z., Harrich, D., Li, Z., Hu, D., Li, D., 2020. Rev. Med. Virol. 31, e2171.
Xia, Y., Chen, Y., Tang, Y., Cheng, G., Yu, X., He, H., Cao, G., Lu, H., Liu, Z., Zheng, S.-Y., 2019. ACS Sens. 4, 3298–3307.
Xue, Q., Wang, Q., Han, Z., Tang, N., Zhou, C., Pan, W., Wang, Y., Duan, X., 2019. Adv. Mater. interfaces 6, 1900671.
Yang, S., Zhang, K., Ricciardulli, A.G., Zhang, P., Liao, Z., Lohe, M.R., Zschech, E., Blom, P.W.M., Pisula, W., Müllen, K., Feng, X., 2018. Angew. Chem. Int. Ed. 57, 4677–4681.
Yao, S., Myers, A., Malhotra, A., Lin, F., Bozkurt, A., Muth, J.F., Zhu, Y., 2017. Adv. Healthcare Mater. 6, 1601159.
Yeh, Y.-T., Tang, Y., Sebastian, A., Dasgupta, A., Perea-Lopez, N., Albert, I., Lu, H., Terrones, M., Zheng, S.-Y., 2016. Sci. Adv. 2, e1601026.
Zhou, C., Zhang, X., Tang, N., Fang, Y., Zhang, H., Duan, X., 2020. Nanotechnology 31, 125302.
Zourob, M., Elwary, S., Turner, A.P., 2008. Principles of Bacterial Detection: Biosensors, Recognition Receptors and Microsystems. Springer Science & Business Media.